Experimental Investigation of MTPA Control of PMSM Drive Employed in Energy-Efficient EV Drive Train

Chiranjit Sain, *Senior Member, IEEE*, Debabrata Mazumdar, Debabsis Chatterjee, and Amarjit Roy, Senior *Member, IEEE*

***Abstract*— The primary goal of this article is to find out best current excitation for controlling maximum torque per amp (MTPA) in internal permanent magnet synchronous motors (IPMSM) with non-sinusoidal back emf. The optimum current elation for the mean torque in the IPMSM is presented in this work in closed form. The suggested work seeks to furnish a universal method for choosing the appropriate current for MTPA control for IPMSM used in EV drive train better than operating vector control for current harmonic injection. Hysteresis current control is also taken into account for current injection in IPMSM. Various examples from experimental investigations are shown, including the optimal current, an FFT analysis of the torque and current profile, and a back emf profile that takes into account the first and third order current harmonics. Finally, this investigation claims an efficient MTPA control strategy under specific operating environment employed in energy-efficient EV drive train.**

***Keywords*— Pulse Width Modulation (PWM), Electric Vehicle, PMSM, MPTA**

I. INTRODUCTION

A revolving electrical machine is termed as PMSM provides a permanent magnet material embedded in its rotor and a balanced three-phase armature placed in its stator. The maintenance issue does not present and the toughness also increases because there is no slide ring-brush arrangement. Typically, the airgap flux distribution and the excitation voltages in the stator windings of a PMSM are created by the permanent magnet material utilized in the PMSM [1]-[2].

The permanent magnet excitation replaces the synchronous machine's traditional field excitation in the rotor, doing away with the need for slip rings and brush assemblies. Due to the improved accessibility of top-quality permanent magnet substances employed in rotor, the PMSM is steadily expanding in industrial acceptability. The primary benefit of the PMSM was thought to be the demagnetization of the permanent magnet materials as a result of the armature reaction brought on by the stator [3–5]. The information about the location of the rotor is used to time the switching of the inverter devices. The inverter is given the idea that it has access to the rotor position data by putting a gray-coded disc on the rotor [8-10]. The need for rotor current to generate the rotor field is removed when there are permanent magnets (PM) on the rotor. In comparison to induction motors of comparable size, operation is more efficient thanks to the elimination of the rotor current. Lower maintenance requirements and the elimination of brush losses are both guaranteed by brushless operation. The main issue with electric vehicles is their constrained driving range because of their finite battery supply. Reducing the losses of the electric drive system utilized in electric vehicles is therefore strongly advised. The field-oriented control method with an optimized direct axis current control and zero direct-axes current component (i.e., id=0). This method does not utilize the IPMSM's reluctance torque since the direct axis-current component is kept at zero, and as a consequence, the torque control is ineffective [6]-[8]. Even while IPMSM drive efficiency has been improved generally by many researchers, there is little research on these techniques for electric vehicles in the literature. Researchers have looked into the use of several motor types in electric vehicles. Given its high efficiency, the PMSM is the favorite solution out of all of them. For PMSM-based EV, many control mechanisms have been suggested. All of these control systems do not place a strong emphasis on the drive system's effectiveness, which is crucial for electric vehicles. All of these control systems do not place a strong emphasis on the drive system's effectiveness, which is crucial for electric vehicles. In order to provide a broad speed-torque range with a limited battery voltage, PMSM for Electric Vehicles is also designed with low inductance winding, which is the cause of the increased harmonic iron loss [9].

The proposed method is executed in a real-time experimental test-bench for the validation once all of the performance characteristics have been considered. Therefore, it is possible to achieve performance with fewer ripples, less noise, and cheaper cost by incorporating machine designs, configuring the position sensor, and the inverter control circuitry [10]. As a result, this suggested architecture is advantageous and suitable for applications in light electric vehicle performance [11–12].

This work proposes a MTPA control strategy for IPMs, which is a contemporary minimizing control approach. Instead of employing traditional vector control, a technique based solely on measuring DC link power is used. In the control application, parameter variation from various sources is also considered [13]-[15].

The remainder of this article is represented in the succeeding manner:

Section-II describes the system representation, Section-III outlines the experimental results and discussion and Section-IV concludes the paper.

C. Sain and A. Roy are with the Department of Electrical Engineering, Ghani Khan Chowdhury Institute of Engineering and Technology, Malda, West Bengal-732141, India (email:chiranjit@gkciet.ac.in, amarjit@gkciet.ac.in). D. Mazumdar and D. Chatterjee are with the Department of Electrical Engineering, NIT Mizoram, Mizoram- 796012, India (email: mazumdardeba@gmail.com, chatterjeedebasis1@gmail.com).

II. SYSTEM REPRESENTATION

The required reference torque is produced by a PI controller in order to reach the desired speed. The effective load torque and drive system losses affect the steady state value of this reference torque. A suitable method is employed to provide a current reference that delivers the necessary torque with the least amount of current. The generalized block diagram of the proposed system is outlined in Fig. 1.

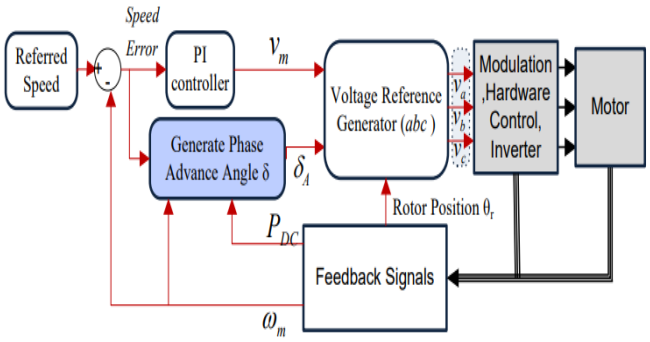

Fig. 1. Generaliized configaration of the proposed system

It is preferable to employ a constant parameter model for the study of an IPM in order to avoid complicated calculations. As a result, the impacts of magnetic saturation and temperature will not be considered during the system's analysis utilizing a constant parameter model. As previously stated, a PI controller is specifically designed to provide the necessary voltage to achieve the specified speed, so regardless of the value of, the matching voltage will be generated by the PI controller automatically. Additionally, it will make implementation simpler because, with constant bus voltage, DC input power measurement only needs one current sensor. Although losses from sources other than copper loss were not considered in the simulation, the MPPA point in the experimental situation would reduce overall motor losses [16]-[19].

The steady-state equations under constant parameter model are described as follows:

$$\begin{bmatrix} V_q \\ V_d \end{bmatrix} = \begin{bmatrix} R & \omega L_d \\ -\omega L_q & R \end{bmatrix} \begin{bmatrix} i_q \\ i_d \end{bmatrix} \quad (1)$$

Using equation (1) q and d-axis voltages are represented as

$$V_q = Ri_q + \omega L_d i_d + \omega \phi_M \quad (2)$$

$$V_d = -\omega L_q i_q + Ri_d \quad (3)$$

At steady-state voltage phasors are characterized by this equation

$$\begin{bmatrix} V_m \cos(\delta) \\ -V_m \sin(\delta) \end{bmatrix} = \begin{bmatrix} R & \omega L_d \\ -\omega L_q & R \end{bmatrix} \begin{bmatrix} i_q \\ i_d \end{bmatrix} + \begin{bmatrix} \omega \phi_M \\ 0 \end{bmatrix} \quad (4)$$

In a similar manner current phasor are described as

$$\begin{bmatrix} i_q \\ i_d \end{bmatrix} = \frac{1}{R^2 + L_q L_d} \begin{bmatrix} R & \omega L_d \\ -\omega L_q & R \end{bmatrix} \begin{bmatrix} V_m \cos(\delta) - \omega \phi_M \\ -V_m \sin(\delta) \end{bmatrix} \quad (5)$$

Further, the q-axis current can be represented as

$$i_q = \frac{1}{R^2 + L_q L_d} \left(RV_m \cos(\delta) - \omega R \phi_M + \omega L_d V_m \sin(\delta) \right) \quad (6)$$

A close examination of the point of minimal current indicates that the phase advance angle that causes MTPA adheres to a predictable pattern. As a result, the proposed control scheme was created in a way that allowed the optimum to be determined based on the operating circumstances.

III. EXPERIMENTAL RESULT & DISCUSSION

The current system consists primarily of an Induction motor coupled with a PMSM, a Motor-Generator set, two front-end converters (FEC-1 and FEC-2), an Inverter-1 for controlling the Induction motor, and an Inverter-2 for controlling the PMSM. The DC bus provides input to concern inverter. Here, if Induction motor is operated in motoring mode then PMSM should be operated in generating mode and vice versa. The selection of the mode is done by the inverter's parameter machine mode. The entire experimental test-bench is presented in Fig. 2.

The suggested approach of the drive system is interfaced using d-SPACE hardware to achieve real-time validation. MATLAB/SIMULINK is used to simulate the driving system. Digital PWM technology is used to manage the drive system in order to obtain the desired performance with reduced jerkiness and smoother operation. Any control method created using MATLAB/Simulink can be applied to a real system using d-SPACE. A few extra libraries are added to the Simulink library browser after installing d-SPACE. These libraries provide with the building blocks needed to connect the d-SPACE to the Simulink program.

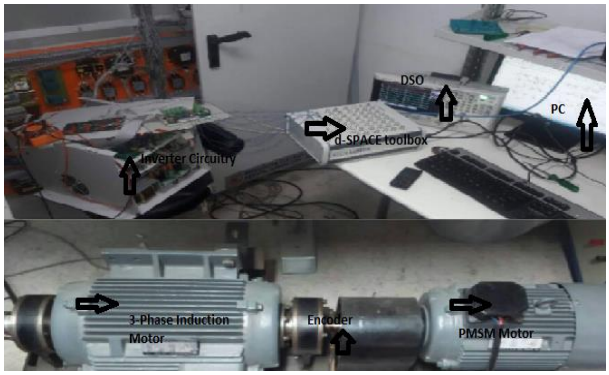

Fig. 2. Fully equipped experimental test bench

Fig. 3. shows the complete detail of the front-end converters' and inverters' internal circuitry. The induction motor is linked to FEC-1 and Inverter-1 in this instance. Moreover, the internal circuit layout of front-end converters and the inverters are outlined in detail. In this platform, the induction motor is connected to FEC-1 and Inverter-1, while the PMSM motor panel is connected to FEC-2 and Inverter-2. The circuit layout for the full hardware setup, including all converter combinations and the sensing system, is shown in Fig. 4.

MicroLabBox was created to be simple to handle in a lab setting. For instance, it can be linked to the mains without the need for a transformer or an additional power source. It gives

external devices common interfaces like Ethernet and USB ports. The board offers analogue and digital input and output channels with built-in signal conditioning for producing and measuring I/O signals. Functional flow diagram is demonstrated in Fig. 5.

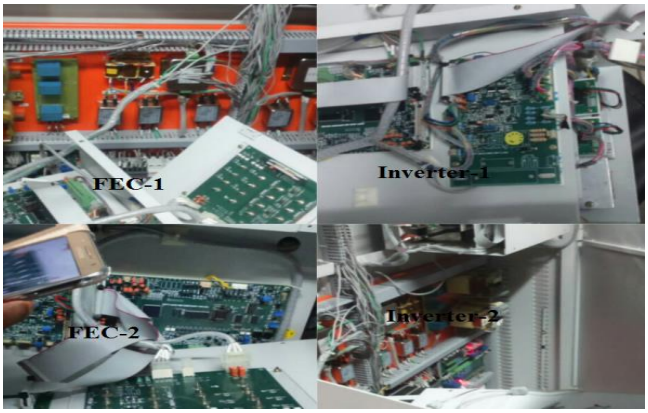

Fig. 3. Layout of the FEC and inverter control panel

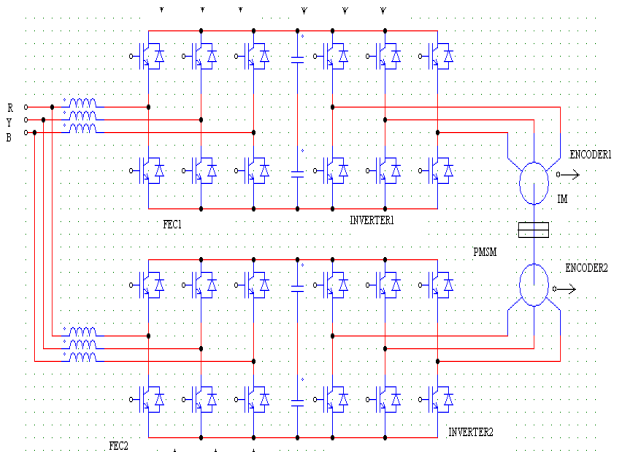

Fig. 4. Circuit layout of hardware set-up

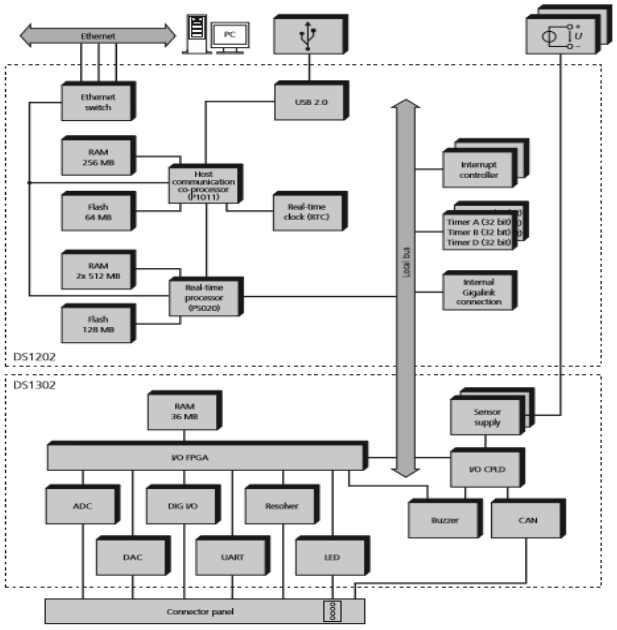

Fig. 5. Functional flow block-diagram of micro lab (d-SPACE) toolbox

By coupling a flywheel and an induction motor to an electrical load operating in constant voltage mode, the speed of the entire system can be stabilised. Hysteresis control is employed to maintain a consistent system speed of 200 RPM while the sinusoidal current with a 1A amplitude serves as the reference. The electrical load's voltage limit is 24 V. The experiment's findings are displayed in Figure. 6.

In this example, the duty cycle of the frond end converter, which is applied to run at the same frequency as PWM for VSI, is regulated to apply pulse width modulation. Without using PWM pulses, the complexity of PWM implementation is reduced, and in addition, switching losses are reduced in comparison to VSI. As illustrated in Fig. 7, it is obvious that using PWM causes a large distortion in the line-to-line voltage and current at the load side when compared to not using PWM for VSI.

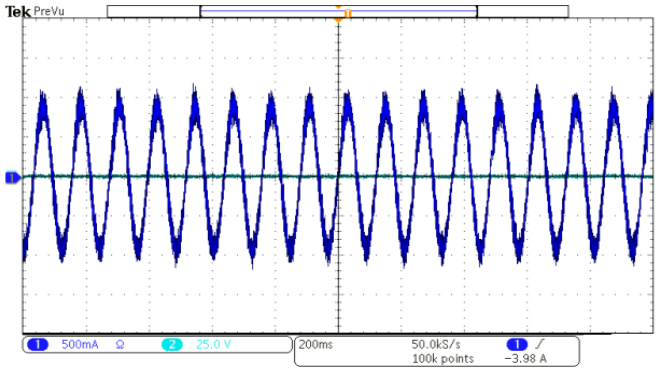

Fig.6. Armature current waveform under MTPA

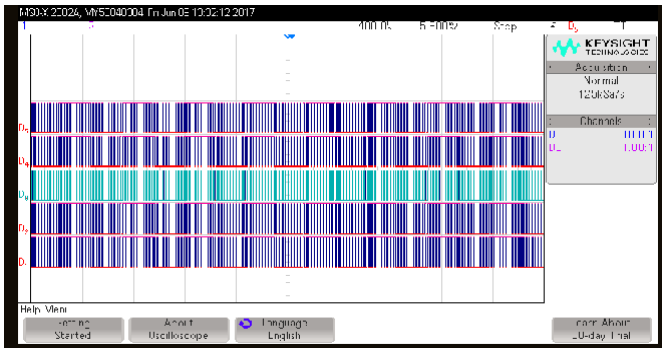

Fig.7. Generation of Digital PWM pulses

An induction motor is used as the prime mover to assess the motor's BEMF; the results of the experiment closely matched those of the theoretical approximation. Back EMF waveform under MTPA enviornment is shown in Fig. 8.

The mechanical outcome from real time setup i.e., torque and speed are well established through Fig.9. and Fig.10. respectively. The generated torque is meant to have a constant value for a specific loading condition because the speed was maintained. Speed response of the motor under load disturbances is depicted in Fig. 10. Load variation on the motor is done in every sample to justify the efficacy of the proposed strategy.

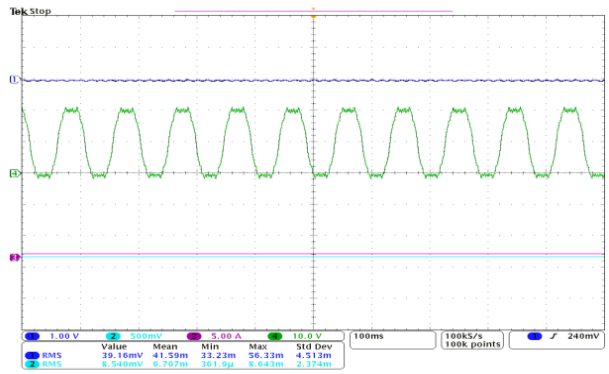

Fig. 8. Tested Back EMF waveform under MTPA

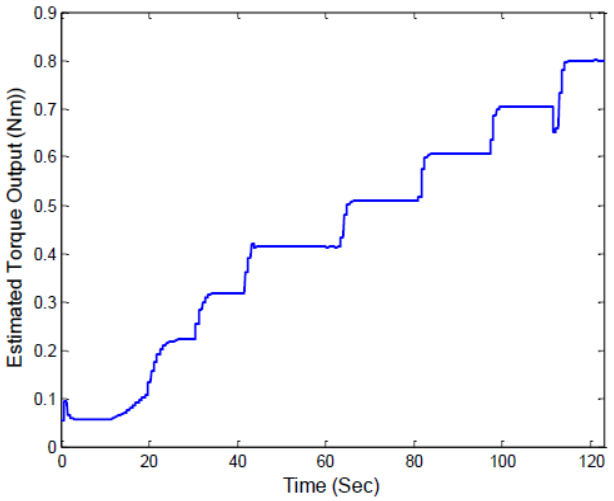

Fig.9. Toque estimation in real-time set up

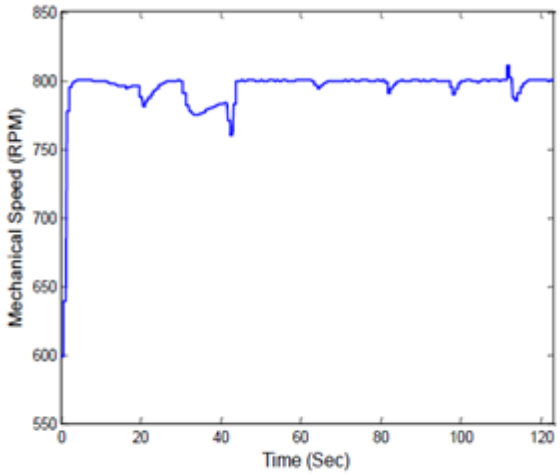

Fig. 10. Speed of the PMSM under load disturbances

Only the first and third order current harmonics should be present in the ideal current since only these two orders of

flux linkage are considered. Otimal variation of current at the peak value is also shown in Fig. 11.

According to Figure 12, injecting appropriate current increased average torque by 1.39%. FFT analysis of the torque profile validates the proposed notion. Figure 12 clearly depicts torque measurement and the FFT analysis.

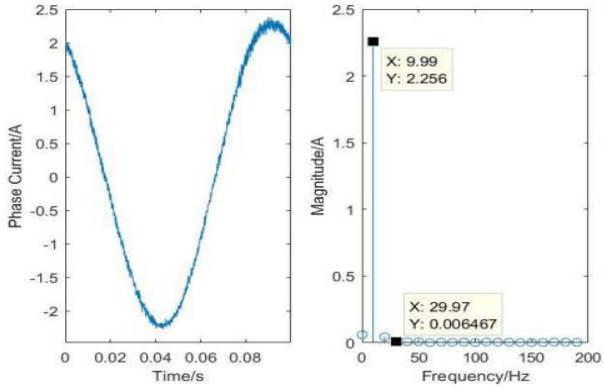

Fig. 11. Otimal variation of current at the peak value

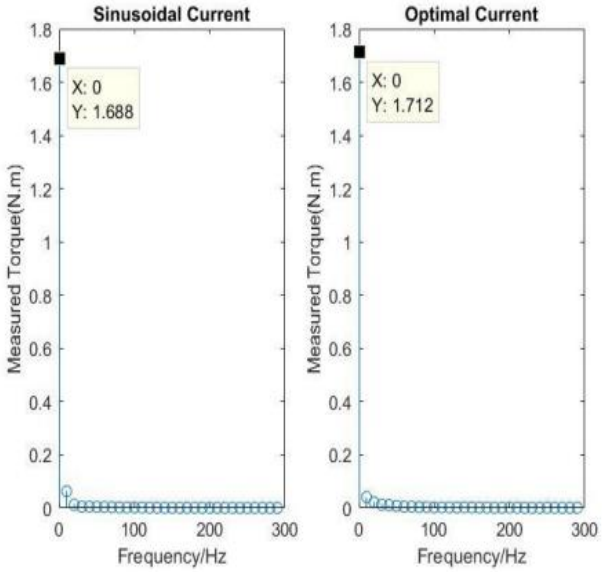

Fig. 12. Torque measurement and FFT analysis

While varying the commanded speed, the load torque was maintained at a constant level to examine how well the algorithm performed at various operating speeds. In Fig. 13 speed of the motor is examined under constant variation of load torque magnitude i.e., 5 Nm. The algorithm is a practical cost-effective solution because the control mechanism is built based solely on the DC link power measurement. The algorithm's self-converging nature makes it resistant to self-induced instability and lowers the possibility of system collapse. Even a slight improvement in electric drive efficiency for electric vehicles is significant since it lengthens their battery life and driving range.

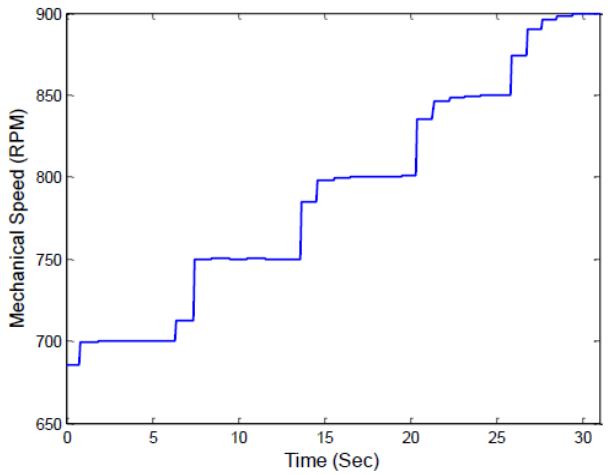

Fig. 13. Speed response under constant load torque magnitude

IV. Conclusion

A variable-equivalent-parameter MTPA control approach based on law has been illustrated. Because the variable-equivalent-parameter MTPA control rule addressed the effects of both motor parameter values and motor parameter derivatives on the MTPA trajectory, the proposed approach may give correct MTPA current references. Furthermore, the aforementioned MTPA control rule eliminates the time-consuming calculations and derivative calculations included in classic MTPA control laws. As a result, the suggested technique can quickly and in real time provide the MTPA with current references. The results of the experiment show that the suggested technique can accurately adjust MTPA under a range of load scenarios and has outstanding dynamic performance. The results of the experiments can be investigated further in this suggested MTPA approach can reduce PMSM stator copper loss. The outcome of this proposed approach can be employed in the EV drive train for enhancing the energy-efficinency in a sustaianable environment.

References

[1] W. Peters, O. Wallscheid, and J. Bocker, "Optimum efficiency control of interior permanent magnet synchronous motors in drive trains of electric and hybrid vehicles," in Proc. of the European Conference on Power Electronics and Applications, pp. 1-10, Sep. 2015.

[2] F. Tinazzi and M. Zigliotto, "Torque estimation in high-efficiency IPM synchronous motor drives," *IEEE Trans. Energy Convers.,* vol. 30, no. 3, pp. 983–990, Sep. 2015.

[3] Z. Tang, X. Li, S. Dusmez, and B. Akin, "A new V/f-based sensor less MTPA control for IPMSM drives," *IEEE Trans. Power Electron.,* vol. 31, no. 6, pp. 4400–4415, Jun. 2016.

[4] Q. Liu, and K. Hameyer, "High-performance adaptive torque control for an IPMSM with real-time MTPA operation," *IEEE Trans. Energy Convers.,* vol. 32, no. 2, pp. 571–581, 2017.

[5] C Sain, A Banerjee, P K Biswas, T Sudhakar Babu, AT Azhar, "Design and Optimization of a Fuzzy-PI Controlled Improved Inverter based PMSM Drive Employed in Light Weight Electric Vehicle," *International Journal of Automation and Control, Inder science Publications*, Vol. 16, Issue 3/4, pp. 459-488, 2022.

[6] S. Li, Y. Li, W. Choi, and B. Sarlioglu, "High-speed electric machines: Challenges and design considerations," *IEEE Trans. Transport. Electrific.* vol. 2, no. 1, pp. 2–13, 2016.

[7] P. Arumugam *et al.*, "High-speed solid rotor permanent magnet machines: Concept and design," *IEEE Trans. Transport. Electrific.,* vol. 2, no. 3, pp. 391–400, 2016.

[8] C. Sain, A. Banerjee, and P K Biswas, "Performance Optimization for Closed Loop Control Strategies towards Simplified Model of a Permanent Magnet Synchronous Motor Drive by Comparing with Different Classical and Fuzzy Intelligent Controllers," *International Journal of Automation and Control, Inderscience Publications*, Vol. 14, No. 4, pp. 469-493, 2020, DOI: 10.1504/IJAAC.2020.10020855

[9] T. Thielemans, J. Vyncke, and J. A. Melkebeek, "Weight factor selection for model based predictive control of a four-level ying-capacitor inverter", *IET Power Electron.,* vol. 5, no. 3, pp. 323-333, 2012.

[10] C Sain, A Banerjee, P K Biswas, and T. Sudhakar Babu, "Updated PSO Optimized Fuzzy-PI Controlled Buck Type Multi-Phase Inverter Based PMSM Drive with an Over-Current Protection Scheme," *IET Electric Power Applications*, Vol. 14, Issue 12, pp. 2331-2339, 2020, DOI: 10.1049/iet-epa.2020.0165.

[11] T. Sun, J. Wang, and M. Koc, "On accuracy of virtual signal injection based MTPA operation of interior permanent magnet synchronous machine drives," *IEEE Trans. Power Electron.,* vol. 32, no. 9, pp. 7405–7408, Sep. 2017.

[12] Z. Yang, F. Shang, I. P. Brown, and M. Krishnamurthy, "Comparative study of interior permanent magnet, induction, and switched reluctance motor drives for EV and HEV applications," IEEE Trans. Transport. Electrific., vol. 1, no. 3, pp. 245–254, 2015.

[13] C. Sain, P. K. Biswas, T. Sudhakar Babu, H. H Alhelou, "Self-Controlled PMSM Drive Employed in Light Electric Vehicle-Dynamic Strategy and Performance Optimization," *IEEE Access*, Vol. 7, pp. 57967-57975, 2021.

[14] A.A. Hassan, and A.M. Kassem, "Modeling, Simulation and Performance Improvements of a PMSM Based on Functional Model Predictive Control," *Arabian Journal of Science and Engineering,* Vol.38, Issue 11, pp.3071-3079, 2013.

[15] C. Sain, A. Banerjee, P. K. Biswas, T. Sudhakar Babu, and B. Chittibabu, "Sensor Angle based Control Strategy and Dynamic Analysis of a Sinusoidal PWM Operated Permanent Magnet Synchronous Machine Drive for Electric Propulsion Unit," *International Transactions on Electrical Energy Systems, Wiley,* Vol 31, issue 12, 2021.

[16] Yoshihiro Miyama, Moriyuki Hazeyama, Shota Hanioka, Norihiro Watanabe, Akihiro Daikoku, and Masaya Inoue, "PWM Carrier Harmonic Iron Loss Reduction Technique of Permanent Magnet Motors for Electric Vehicles," *IEEE Transactions on Industry Applications,* vol. 99, no. 1, pp. 1–7, 2016.

[17] P. Chen, R. Tang, W. Tong; X. Han, J. Jia, and X. Zhu, "Analysis of losses of permanent magnet synchronous motor with PWM supply," in Proc. *Int. Conf. Elect. Mach. Syst*, pp. 1119–1124, 2014.

[18] H. C. Chen and H. H. Huang, "Design of buck-type current source inverter fed brushless DC motor drive and its application to position sensorless control with square-wave current," *IET Elect. Power Applicat,.* vol. 7, no. 5, pp. 416–426, 2013.

[19] M. Nasir Uddin, Hon Bin Zou, F. Azevedo, "Online loss minimization based adaptive flux observer for direct torque and flux control of PMSM drive," In *IEEE Transactions on Industry Applications*, Vol. 52, issue. 1, 2016.